A Random Capillary Model with Application to Char Gasification at Chemically Controlled Rates

Porous particles are described by a random capillary model predicting the frequency of pore intersections and the evolution of pore volume and surface area during reaction. The model is applied to char gasification at chemically controlled rates, and the results are compared with data from the literature.

GEORGE R. GAVALAS

Division of Chemistry and Chemical Engineering
California Institute of Technology
Pasadena, California 91125

SCOPE

Random capillary models have been used widely to describe catalytic and noncatalytic reactions in porous particles. In these applications, it has not been necessary to precisely elaborate the random nature of the capillary structure. In particular, the overlap volume and number of intersections between different capillaries was either ignored or treated in an ad hoc fashion. Overlap volume is the key concept for describing the changing pore volume and surface area in reactions such as char gasification. Likewise, the frequency of intersections is often required to describe mass transfer in coals and chars when an effective diffusivity is not applicable.

In this paper, we develop a random capillary model in which number of intersections, length of pore segments and evolution of pore volume and surface area are exactly and consistently derived from a single probability-density function characterizing the porous solid. As an application of the model, we analyze the gasification of char by oxygen or other gases under conditions of chemical control of the reaction rate. An expression is obtained for the conversion-time curve which clearly displays the effects of surface reaction rate and porous structure. In addition to these model-specific results, we obtain some general model-independent results concerning char conversion. Both the model dependent and the general results are compared with experimental data from the literature.

The random capillary model which is here applied and tested for chemically controlled reaction rates could be applied to char reactions involving diffusional limitations. However, the resulting equations would require numerical solution. In all applications, the assumption of constant reactivity of the pore surface should be kept in mind. This assumption should be further tested experimentally. A simple application of the random model to coal pyrolysis was given recently by Gavalas and Wilks (1979).

CONCLUSIONS AND SIGNIFICANCE

A random capillary model has been developed describing the porous medium by a single density function $\lambda(R)$, related but not identical to the customary pore size distribution. Precise expressions are derived for the number of intersections between pores of different sizes, the lengths of the pore segments between intersections and the evolution of pore volume and surface area accompanying pore enlargement by reaction.

An application to char gasification by oxygen (or carbon dioxide, water, hydrogen) is considered under two assumptions: no diffusional limitations and no dependence of the intrinsic surface reaction rate on conversion. First some general, model-independent results are obtained. It is shown that for any given char, the conversion curves $x_c(t)$ corresponding to different temperatures, pressures and reacting gases reduce to a single master curve if plotted against a suitable dimensionless time. Moreover, the rate vs. conversion curves (dx_c/dt vs. x_c) can be reduced to a single curve by suitable scaling of the rate dx_c/dt. In particular, the conversion x_{cm} at which the dx_c/dt attains its maximum is independent of reacting gas and temperature.

Using the random capillary model, the following expression for $x_c(t)$ is derived:

$$x_c(t) = 1 - \exp[-2\pi(B_0 v^2 t^2 + 2B_1 v t)]$$

Comparison with experimental data from the literature show that the model independent results concerning the master curves for x_c, dx_c/dt are obeyed quite well at sufficiently low temperatures. Some deviations observed, especially for gasification by carbon dioxide, are attributed either to diffusional limitations or to the catalytic effect of mineral matter which may interfere with the second assumption about the constancy of the surface reaction rate. The specific expressions for $x_c(t)$ and dx_c/dt derived from the random capillary model described quite well experimental data of char gasification by oxygen up to $x_c = 0.7$. These comparisons require the adjustment of only two parameters: $B_0 v^2$, $B_1 v$. In the Appendix, some results of the model are used to derive an approximate criterion for the absence of diffusional limitations.

It may be justifiably argued that the porous structure of chars deviates from the random capillary model because of noncylindrical pores and possible spatial regularities. Such deviations will affect the detailed form of the conversion-time curve. However, the results of the model concerning pore intersections and overlap and the general characteristics of the conversion curve are believed to be at least qualitatively correct. The effect of deviations from random cylindrical capillaries can probably be absorbed in the two parameters B_0, B_1.

0001-1541-80-3900-0577-$01.05.

Capillary models have been widely applied to the problem of reaction and diffusion in porous materials, either catalyst pellets of particles consumed by the reaction. Diffusion in porous catalyst pellets has been treated by Johnson and Stewart (1965) and Feng and Stewart (1973) by a capillary model postulating thorough cross linking, random pore orientation and a distribution of pore radii. For the porosities encountered in catalyst pellets, the length of pore segments between intersections must be only a small multiple of pore radius, a fact having the following two implications: the flux relationships for an infinite capillary are not strictly applicable and a significant fraction of the pore space cannot be assigned to a single capillary but is an overlap region shared by two or more capillaries. This fact, in turn, introduces considerable ambiguity in the interpretation of experimental porosimetry and surface area data in terms of the capillary model. Such defects of the customary capillary model are not too restrictive from the standpoint of diffusion in catalyst pellets inasmuch as deviations from the infinite cylindrical shape can be generally incorporated in an adjustable parameter, the tortuosity, or in other adjustable parameters as in the work of Feng and Stewart (1973).

The modeling of diffusion and reaction in porous materials that are consumed by the reaction is more difficult because of the transient nature of the porous structure. In an early paper, Petersen (1957) treated diffusion and reaction in a single cylindrical capillary and in a random assembly of capillaries of the same radius. Recognizing the importance of pore intersections and overlap, he introduced two parameters to express the surface area as a function of pore radius and derived a relationship between porosity and surface area. However, the number and geometry of intersections were not linked to the random geometry of the capillaries, and as a result the expressions derived for porosity and surface area are largely empirical.

Szekely and Evans (1970, 1971) used two structural models to describe reaction and diffusion in porous solids. Their pore (or capillary) model postulated parallel pores of uniform size. In the limit of kinetic control, this model predicts that the overall reaction rate attains a maximum at an intermediate conversion, although the uniform size and the parallel location of the pores are rather restrictive assumptions. The other structural model, the one used in most of their later work, is the grain model wherein the porous medium is described as a collection of spheres, possibly of different sizes. In the limit of chemical control, this model would predict a monotonically decreasing reaction rate and would thus seem inadequate for describing char gasification where the reaction rate is often observed to display a maximum. The grain model has been successfully applied to oxide reduction and other metallurgical reactions.

A random pore model was also proposed by Hashimoto and Silveston (1973) and applied to char gasification. The change in the pore structure is described by a population balance equation involving five to ten parameters. By adjusting these parameters, good agreement was obtained with experimental data. A related but more refined random capillary model of char was recently formulated by Simons and Finson (1979) and Simons (1979). The model deals with important quantities such as density of pore intersections, the length of pore segments, etc. However it does not relate these quantities to the fundamental pore statistics by first principles and is thus forced to utilize several empirical relations.

Char gasification is a very important and intriguing example of reactions in which the overall rate is strongly influenced by the porous structure of the solid. Most experimental studies, especially in combustion, involve conditions of diffusional limitations. However, a number of studies have utilized sufficiently low temperatures such that the reaction was either under chemical control or just above the threshold of diffusional limitations. Jenkins et al. (1973), Hippo and Walker (1975), Linares et al. (1979), Tomita et al. (1977), Mahajan and Walker (1979) and Mahajan et al. (1978) studied the low temperature reactions of various chars with oxygen, carbon dioxide, water and hydrogen with the objective to clarify the role of pore structure, rank, heat treatment and mineral matter on char reactivity. Dutta and Wen (1977) and Dutta et al. (1977) studied the reactivity of various chars to oxygen and carbon dioxide, respectively. These studies provide a wealth of information relating to the multitudinous factors affecting char reactivity and are suitable for testing various pore models.

THE RANDOM CAPILLARY MODEL

In this model, the porous structure is assumed to consist of infinitely long, straight, cylindrical capillaries (or pores) with radii in a range $R_* \leq R \leq R^*$. The axes of the capillaries are located completely randomly, that is, without any anisotropy or spatial correlations. The term random has intuitive appeal but needs a precise mathematical definition, otherwise it can lead to subtle but serious errors.

The random spatial distribution of geometric objects such as straight lines is a mathematical problem of long standing reviewed in a monograph by Kendall and Moran (1963). Here we only need a few principles that can be introduced informally as follows.

A straight line is specified by four numbers: its intersection (x,y) with a fixed plane and its orientation defined by two angles: θ, the angle with the normal to the plane, and ϕ, the aximuthal angle. The probability density must be uniform and isotropic in space; therefore (x,y) and (θ,ϕ) must be distributed independently. Moreover, the density of (x,y) must be a two-dimensional Poisson process with mean λ; that is, λdS is the probability of a single intersection in a surface element dS as $dS \to 0$. This probability density must be independent of the reference plane; therefore the same probability λdS applies to any surface element dS in space. The probability of orientation can be found by the following invariance argument. Consider two arbitrary oriented elements in space dS_1, dS_2 centered as $\underline{x}_1$, $\underline{x}_2$ with unit normals $\underline{n}_1$, $\underline{n}_2$ as shown in Figure 1*a*. The expected number dN_{12} of lines emanating from dS_1 and reaching dS_2 is given by

$$dN_{12} = \lambda dS_1 \, P(\underline{n}_1, \underline{x}_2 - \underline{x}_1) \, d\Omega_{12}$$

where $d\Omega_{12}$ is the solid angle at $\underline{x}_1$ subtended by dS_2 and P is the orientational probability density. The corresponding number dN_{21} is

$$dN_{21} = \lambda dS_2 \, P(\underline{n}_2, \underline{x}_1 - \underline{x}_2) \, d\Omega_{21}$$

The solid angles are given by

$$d\Omega_{12} = dS_2 \frac{(\underline{x}_2 - \underline{x}_1) \cdot \underline{n}_2}{|\underline{x}_2 - \underline{x}_1|^2}$$
$$d\Omega_{21} = dS_2 \frac{(\underline{x}_1 - \underline{x}_2) \cdot \underline{n}_1}{|\underline{x}_2 - \underline{x}_1|^2} \qquad (1)$$

The numbers dN_{12}, dN_{21} must be equal, however, because the straight lines concerned are the same. It follows that

$$(\underline{x}_2 - \underline{x}_1) \cdot \underline{n}_2 \, P(\underline{n}_1, \underline{x}_2 - \underline{x}_1) = (\underline{x}_2 - \underline{x}_1) \cdot \underline{n}_1 \, P(\underline{n}_2, \underline{x}_1 - \underline{x}_2) \qquad (2)$$

To satisfy this condition for all $\underline{n}_1$, $\underline{n}_2$ we must have

$$P(\underline{n}, \underline{x}_2 - \underline{x}_1) = \frac{1}{\pi} \underline{n} \cdot (\underline{x}_2 - \underline{x}_1) = \frac{1}{\pi} \cos(\underline{n}, \underline{n}_2 - \underline{x}_1) \qquad (3)$$

where $1/\pi$ is the normalization constant such that the integral of dN_{12} over all solid angles on the one side of the element dS_1 (the other side includes the same lines) is equal to λdS_1.

Equation (3), the cosine law, is familiar from thermal radiation theory, where it is called Lambert's law, and from neutron transport theory. The above argument is equivalent to a more formal derivation utilizing the invariance of the probability density function with respect to rotations. The probability density function is now precisely established and is fully specified by the parameter λ.

We now have the tools to derive a number of fundamental results concerning the porous medium. To start with, we consider pores of uniform radius R and establish the connection between the porosity ϵ and the parameter λ. Any point in space belongs to the solid portion of the medium if it is at distance R or larger from the axes of all pores. Hence $1 - \epsilon$ is the probability that a sphere of radius R is not intersected by any of the randomly distributed pore axes. Figure 1*b* shows how to compute this probability. The sphere S is surrounded by a concentric sphere S_L of radius $R_L >>> R$. All lines intersecting S must originate at the surface of S_L. The lines originating from an element dS_L and intersecting the sphere S are given by

$$dN = \frac{\lambda}{\pi} dS_L \Omega$$

where Ω is the solid angle subtended by the sphere S and the cosine is equal to one in the limit $R_L \to \infty$. In the same limit, the solid angle is given by

$$\Omega = \frac{\pi R^2}{R_L^2}$$

so that

$$dN = \lambda \left(\frac{R}{R_L}\right)^2 dS_L$$

The probability that no line emanating from dS_L intersects S is clearly

$$p(dS_L) = e^{-dN} \tag{4}$$

according to the properties of the Poisson density. Since the probabilities corresponding to different elements dS_L are independent, the probability of no intersection is

$$1 - \epsilon = \Pi\, p(dS_L) = \exp(-\int dN)$$

where the product and integral are taken over all elements dS_L in the upper hemisphere. Elements in the southern hemisphere do not contribute additional lines since each intersecting line belongs to two diametrically opposed elements dS_L. Using (4), we obtain the fundamental relationship

$$1 - \epsilon = \exp(-2\lambda\pi R^2) \tag{5}$$

$$\lambda = \frac{1}{2\pi R^2} \ln\left(\frac{1}{1-\epsilon}\right) \tag{6}$$

In the case of porous media with uniform sized pores, Equation (6) can be used to determine the parameter λ from experimental data. According to Equation (6), as $\epsilon \to 1$ (fixed R), $\lambda \to \infty$, a result that is not physically meaningful. The random pore model is evidently unsuitable for highly porous media which could be better described as randomly located solid cylinders. This limitation of the random pore model should be kept in mind in the applications discussed later. For small values of ϵ (or λ), Equation (6) gives

$$\epsilon \cong 2\lambda\pi R^2 \tag{7}$$

Another useful quantity is the total length l of pore axes per unit volume. This can be derived from the porosity in the limit $R \to 0$ (constant λ):

$$l = \lim_{R\to 0} \frac{\epsilon}{\pi R^2} = 2\lambda \tag{8}$$

For finite R, $\epsilon < \pi R^2 l$ because of pore overlap.

We next consider the number of intersections among pores. The number of intersections per unit length of a given pore is obtained by considering a coaxial cylinder of radius $2R$. The number of intersections of pore axes with this cylinder per unit length of the cylinder is

$$n' = \frac{2\pi(2R)\lambda}{2} = 2\pi R\lambda \tag{9}$$

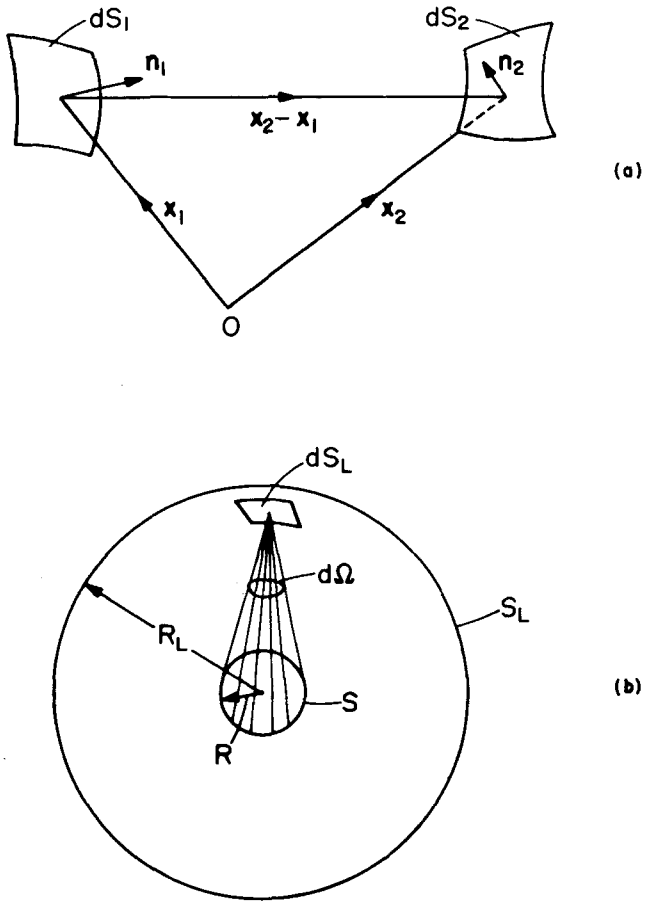

Figure 1. Derivation of fundamental relations: (a) orientational probability (b) porosity

where the factor 2 in the denominator takes into account that each pore axis intersects the cylinder at two points. The number of intersections per unit volume is then

$$n = \frac{2\lambda n'}{2} = 2\pi R\lambda^2 \tag{10}$$

where the factor 2 at the denominator is again needed to avoid double counting.

The foregoing results can be extended to the case of a discrete or continuous pore size distribution. To be definite, we examine the latter case with the pore radius varying in an interval $[R_*, R^*]$. Assuming that pores of different sizes are distributed in space independently, we define $\lambda(r)dR$ to be the density of intersections of pores with radius in $[R, R + dR]$ with any surface element. As before, the probability that a point does not belong to the volume occupied by capillaries with radii in $[R, R + dR]$ is

$$\exp[-2\pi\lambda(R)R^2 dR]$$

The probabilities corresponding to different elements dR are independent; therefore

$$\exp[-2\pi\textstyle\int_R^{R^*} \lambda(R')R'^2 dR']$$

is the probability that a point does not belong to the volume occupied by capillaries having radius in $[R, R^*]$. The quantity

$$F(R) = 1 - \exp[-2\pi \textstyle\int_R^{R^*} \lambda(R')R'^2 dR'] \tag{11}$$

is the probability that a point belongs to the space of capillaries with radius in $[R, R^*]$. F also represents the volume of capillaries $[R, R^*]$, including the overlap volume with smaller capillaries. The total pore volume is

$$\epsilon_T = F(R_*) = 1 - \exp\left[-2\pi \int_{R_*}^{R^*} R^2\lambda(R)dR\right] \tag{12}$$

Within the framework of the random pore model, the density $\lambda(R)$ can be determined from porosimetry data obtained from mercury penetration or nitrogen desorption (adsorption). Consider, for example, the latter case, and let $\epsilon(R)\,dR$ be the experimental pore volume fraction in $[R,R+dR]$. As customarily defined from experimental data, $\epsilon(R)$ does not involve overlap; that is, $\int\epsilon(R)\,dR$ is the total pore volume.

Consider the determination of pore size distribution from the desorption branch of the nitrogen isotherm. At a pressure level p the volume of pores of radius $R(p)$ and larger are empty, where $R(p)$ is given by Kelvin's equation. This volume includes the overlap with smaller pores; therefore it is equal to $F(R)$. When the pressure is reduced to $p-dp$, an additional volume element $\epsilon(R)dR$ is emptied, where

$$\epsilon(R)|dR| = F(R) - F(R+dR)$$

Therefore

$$\epsilon(R) = -\frac{dF}{dR} \tag{13}$$

Integrating with the initial condition $F(R^*)=0$, we find

$$F(R) = \int_R^{R^*}\epsilon(R')dR' \tag{14}$$

Differentiating Equation (11) and using (13) and (14), we obtain the relationship between $\lambda(R)$ and the experimental pore size density $\epsilon(R)$:

$$\epsilon(R) = 2\pi R^2\lambda(R)\exp\left[-2\pi\int_R^{R^*}R'^2\lambda(R')dR'\right] \tag{15}$$

$$\lambda(R) = \frac{1}{2\pi R^2}\frac{\epsilon(R)}{1-\int_R^{R^*}\epsilon(R')dR'} \tag{16}$$

For low porosities, we have the approximate relationship

$$2\pi R^2\lambda(R) \cong \epsilon(R) \tag{17}$$

which can be used for coals and chars, before significant burn-off has taken place, since the initial porosity (excluding the microporosity) is usually quite low (<0.1).

Certain applications require information about pore connecticity, that is, the frequency of intersections between pores of different sizes. The number of intersections of pores of radius R (R pores) with pores having radius in an interval $[R',R'+dR']$ can be found as follows. Consider an R pore and a coaxial cylinder C of radius $R+R'$. All R' pores with axes piercing C intersect the R pore. The number of intersections per unit length of C is, as before

$$\frac{2\pi(R+R')\lambda(R')dR'}{2}$$

The number of intersections with pores in $[R',R'+dR']$ per unit length of an R pore is

$$n'(R,R')dR' = \pi\lambda(R')(R+R')dR' \tag{18}$$

while the number of intersections per unit volume between pores in $[R,R+dR]$ and pores in $[R',R'+dR]$ is

$$n(R,R')dRdR' = 2\pi\lambda(R)\lambda(R')(R+R')dRdR' \tag{19}$$

A related quantity is the probability that a segment of an R pore of length L is not intersected by pores in the range $[R',R+dR']$. This probability follows immediately from the properties of the Poisson density as

$$p(R,R')dR' = \exp\left[-Ln'(R,R')dR'\right] \tag{20}$$

Of more interest is the probability $p(R)$ of no intersection by pores of radius larger than R, which is given by

$$p(R) = \exp\left[-L\int_R^{R^*}n'(R,R')dR'\right] \tag{21}$$

Corresponding to $p(R)$ there is a mean length of R pore segments between intersections with larger pores. This is given by

$$L(R) = \int_0^\infty p(L)dL = \left[\int_R^{R^*}n'(R,R')dR'\right]^{-1} \tag{22}$$

The above results carry with little modification to a discrete distribution with radii $R_1,\ldots,R_n$. The number of intersections $i-j$ per unit length of the i pores is

$$n'_{ij} = \pi\lambda_j(R_i+R_j) \tag{23}$$

while the number of such intersections per unit volume is

$$n_{ij} = \begin{cases}2\pi\lambda_i\lambda_j(R_i+R_j) & i\neq j\\ \pi\lambda_i\lambda_j(R_i+R_j) & i=j\end{cases} \tag{24}$$

For an i pore segment of length L, the probability p_i of no intersections with pores i or larger and the probability of no intersections with pores larger than i are

$$p_i(L) = \exp\left(-L\sum_{j=1}^{n}n'_{ij}\right) \tag{25}$$

$$p'_i(L) = \exp\left(-L\sum_{j=i+1}^{n}n'_{ij}\right) \tag{26}$$

The corresponding mean lengths of segments between intersections are

$$L_i = \int_0^\infty p_i(L)LdL = \left(\sum_{j=1}^{n}n'_{ij}\right)^{-1} \tag{27}$$

$$L'_i = \int_0^\infty p'_i(L)LdL = \left(\sum_{j=i+1}^{n}n'_{ij}\right)^{-1} \tag{28}$$

CHAR GASIFICATION AT CHEMICALLY CONTROLLED RATES

In this section we apply the random pore model to the chemically controlled gasification of char by oxygen, carbon dioxide, or steam. Before proceeding with the analysis, we need to clarify the meaning of the term chemical control. Coals and chars have a very broad size distribution which is suitably (Gan et al., 1972) divided into three ranges, the micropores ($R<6\times10^{-4}\,\mu$m), the transitional pores ($6\times10^{-4}<R<1.5\times10^{-2}\,\mu$m) and the macropores ($1.5\times10^{-2}<R\leq1.5\,\mu$m). The distinction between micropores and transitional pores is made on the basis of the change from very slow activated diffusion to Knudsen diffusion. Since the type of diffusion depends on the size, shape and polarity of the diffusing molecules, the radius marking the transition from activated to Knudsen diffusion depends on the diffusing gas so that the radius $6\times10^{-4}\,\mu$m listed as an upper bound of micropore size is only indicative. On the other hand, the radius $1.5\times10^{-2}\,\mu$m marking the division between transitional pores and macropores relates to the different porosimetry techniques used in the two size ranges and is not of particular significance.

At this point we introduce the assumption that the contribution of the micropores to the overall reaction rate when reduced to unit surface area of transitional pores and macropores is independent of conversion. This assumption cannot be directly assessed, although it can be intuitively interpreted as follows. Because of the very slow activated diffusion, the reaction in the micropores occurs in a small region near the point where the micropore intersects a transitional pore or macropore. As the surface of the latter pores recedes owing to the reaction, new micropore area is exposed such that the reaction rate due to the micropores, per unit area of the larger pores, is constant. The contribution of the micropore surface may, in some cases, be small. Dutta et al. (1977) have found that the rate of char gasification by carbon dioxide is approximately proportional to the surface area of pores $15\times10^{-4}\,\mu$m and larger. The difference between this and the $6\times10^{-4}\,\mu$m radius which customarily defines the upper size of micropores may be due at least partly to the low area in the range 6×10^{-4} to $10\times10^{-4}\,\mu$m or the difficulty in measuring surface area in this range by the nitrogen adsorption-desorption technique.

While diffusion in the micropores is assumed to be so slow that the micropore surface area makes a constant contribution to the reaction rate, diffusion in the transitional and macropores is assumed to be very fast. Hence, all surface area corresponding to macropores and transitional pores is exposed to a uniform concentration of reactant gases. These are then the conditions for chemically controlled rates. In the Appendix we derive some approximate criteria for the absence of diffusional limitations.

We now consider the evolution of pore structure due to reaction. Let the surface reaction rate be

$$r(c,c_s,T)$$

in grams of carbon per unit area and time, where r is a function of the temperature T, the concentration c of the reactant gas and the concentration c_s of active sites which incorporates the effective concentration of mineral catalysts. This rate is expressed per unit area of transitional pores and macropores and includes the contribution of micropores, if any. Both c and c_s may actually involve several concentrations. If the apparent (mercury) density of carbon in the char is ρ_c, then $\rho_s = \rho_c/(1-\epsilon_T)$ is the density in the portion of the volume excluding transitional pores and macropores. The density ρ_s is constant as a result of the above assumption about reaction in the micropores. The velocity with which a pore surface element recedes owing to reaction is

$$v(c,c_s,T) = \frac{1}{\rho_s} r(c,c_s,T) \tag{29}$$

The additional assumption is now introduced that c_s, the surface concentration of active sites, including the catalytic sites, does not change with the progress of the reaction. The validity of this assumption clearly depends on the distribution of mineral matter, especially calcium and magnesium minerals which have been shown by Jenkins et al. (1973), Linares et al. (1979) and Mahajan and Walker (1979) to be mainly responsible for the catalytic activity. Evidently, the magnitude of the catalytic effect and its implications relative to the last assumption depends both on the particular char and the reaction considered.

The above assumptions of constant contribution of the micropores, constant c_s and uniform c (no diffusional limitations) implies that v is a quantity that depends on T, c and the particular reaction but does not depend on the carbon conversion (or burn-off) x_c. The constancy of v leads by a simple argument to some general results about conversion, independent of any assumptions about the porous structure. The evolving pore surface can be abstractly defined just like any surface in three dimensional space as

$$S(\underset{\sim}{x},t) = 0$$

which yields, by differentiation

$$S_t + \nabla_x S \cdot \frac{d\underset{\sim}{x}}{dt} = 0$$

If $n(\underset{\sim}{x})$ is the outward normal at a point $\underset{\sim}{x}$ on the pore surface

$$\frac{d\underset{\sim}{x}}{dt} = -v\underset{\sim}{n}$$

But $\underset{\sim}{n} = \nabla_x S$; therefore, introducing in the differential equation, we obtain

$$S_t - v|\nabla_x S| = 0$$

Using any characteristic length L_c we can rewrite the above equation in the dimensionless variables $\underset{\sim}{x}' = \underset{\sim}{x}/L_c$, $t' = tv/L_c$

$$S_{t'} - |\nabla_{x'} S| = 0$$

Therefore, the equation for the surface must actually be

$$S = S\left(\frac{\underset{\sim}{x}}{L_c}, \frac{tv}{L_c}\right) \tag{30}$$

The pore surface area, the pore volume and the conversion are clearly universal functions of tv/L_c; for example

$$x_c = X\left(\frac{tv}{L_c}\right) \tag{31}$$

The functional relationship, Equation (31), could have been obtained by similarity arguments, without the above formal derivation. From Equation (31) follow a number of important conclusions:

1. For a given char, conversion-time curves corresponding to different reacting gases, pressures and temperatures can be reduced to a single master curve by using the dimensionless time $t' = tv/L_c$. Since v is usually unknown, it is better to define a different dimensionless time as follows. Let $t_{0.5}$ be the time at $x_c = 0.5$. From (31)

$$t_{0.5} = \frac{l_{0.5}}{v}$$

where $l_{0.5}$ is a constant characteristic of the inital pore structure. Although $l_{0.5}$, v are unknown, $t_{0.5}$ can be measured experimentally. Using the dimensionless time $t'' = t/t_{0.5}$, we have

$$x_c = X\left(\frac{l_{0.5}}{L_c} t''\right)$$

Therefore, all curves again reduce to a single master curve. This reduction can be obviously accomplished using any time corresponding to a fixed conversion level. Since $v \propto 1/t_{0.5}$, by measuring $t_{0.5}$ at different temperatures and pressures of the reactant gas we can determine the experimental activation energy and the reaction order.

2. The reaction rate per unit initial weight is

$$\frac{dx_c}{dt} = \frac{v}{L_c} X'\left(\frac{tv}{L_c}\right) \tag{32}$$

where prime indicates derivative.

Eliminating tv between (31) and (32), we obtain

$$\frac{dx_c}{dt} = \frac{v}{L_c} G(x_c) \tag{33}$$

where G is characteristic of the char but independent of reactant gas and temperature. Equation (33) implies that dx_c/dt vs. x_c curves corresponding to different reactions, temperatures, etc., can be all reduced to a single curve by appropriate scaling of dx_c/dt. A special result is that if dx_c/dt has a maximum, it is attained at a conversion x_c independent of T, etc., but dependent on the char in question. Equation (33) also states that the maximum rate $(dx_c/dt)_m$ is proportional to the reaction velocity v; therefore it too can be used for determining the experimental activation energy and reaction order.

This is as far as we can go without commitment to a specific pore model. We now proceed to derive the functional form of x_c, dx_c/dt for the random capillary model. We denote by $q(t)$ the increase in the radius of any capillary in the time from zero to t; that is

$$R(t) = R_0 + q(t) \tag{34}$$

The radius of the char particle decreases by the same amount:

$$R_p(t) = R_{p0} - q(t) \tag{35}$$

The probability density function at time t is given in terms of the original probability density function λ_0

$$\lambda(R,q) = \lambda_0(R - q) \tag{36}$$

so that the total pore volume is

$$\epsilon_T(q) = 1 - \exp\left[-2\pi \int_{R_*}^{R^*} (R_0 + q)^2 \lambda_0(R_0) dR_0\right] \tag{37}$$

which may be rewritten as

$$\frac{1-\epsilon_T(q)}{1-\epsilon_{T0}} = \exp[-2\pi(B_0 q^2 + 2B_1 q)] \tag{38}$$

where

$$B_0 = \int_{R_0^*}^{R_0^*} \lambda(R_0) dR_0 \tag{39}$$

$$B_1 = \int_{R_0^*}^{R_0^*} R_0 \lambda(R_0) dR_0 \tag{40}$$

The zeroth moment B_0 is the total number of capillary axes intersecting a unit surface area, while the first moment B_1 is equal to the product of B_0 and the mean pore radius.

As q increases by a length dq, the pore volume increases by $d\epsilon_T = S(q)dq$, where $S(q)$ is the total pore surface area. Hence

$$S(q) = \frac{d\epsilon_T}{dq} = 4\pi[1 - \epsilon_T(q)](B_0 q + B_1) \tag{41}$$

Pore volume and surface area have now been expressed as functions of a single variable q.

The conversion, or burn-off, x_c is defined by the amount of carbon reacted divided by the initial amount of carbon; that is

$$x_c(q) = 1 - \left(1 - \frac{q}{R_{p0}}\right)^3 \frac{1 - \epsilon_T(q)}{1 - \epsilon_{T0}}$$

and using Equation (38), we set

$$x_c(q) = 1 - \left(1 - \frac{q}{R_{p0}}\right)^3 \exp[-2\pi(B_0 q^2 + 2B_1 q)] \tag{42}$$

Under conditions of chemical control it can be shown that $q \lll R_{p0}$. For the purpose of an order of magnitude estimate we consider capillaries of uniform initial size R_0. If λ is the number density of pore mouths on any surface, $1/\lambda^{\frac{1}{2}}$ is the spacing of pore mouths. At complete conversion, $q \sim 1/\lambda^{\frac{1}{2}}$. For small ϵ_0, $\lambda = \epsilon_0/2\pi R_0$ so that

$$\frac{q}{R_{p0}} \sim \left(\frac{2\pi}{\epsilon_0}\right)^{\frac{1}{2}} \frac{R_0}{R_{p0}} \tag{43}$$

Assuming that some transitional porosity exists and taking $\epsilon_0 = 0.01$ and $R_0 = 5 \times 10^{-3}\ \mu$m, $R_{p0} = 50\ \mu$m, we find $q/R_{p0} \sim 2.5 \times 10^{-3}$.

Neglecting the term due to the slight change in the particle size, we obtain the basic expression

$$x_c(t) = 1 - \exp[-2\pi(B_0 q^2 + 2B_1 q)] \tag{44}$$

When the temperature and concentration of reacting gases remain constant and the pore surface maintains constant reactivity, we have

$$q = vt$$

where v is a constant given by Equation (29). Then

$$\frac{dx_c}{dt} = 4\pi(B_0 v^2 t + B_1 v) \exp[-2\pi(B_0 v^2 t^2 + 2B_1 vt)] \tag{45}$$

Eliminating t between (44) and (45), we obtain the relation between reaction rate and conversion:

$$\frac{dx_c}{dt} = 4\pi(1 - x_c)\left[(B_1 v)^2 + \frac{B_0 v^2}{2\pi} \ln\left(\frac{1}{1 - x_c}\right)\right]^{\frac{1}{2}} \tag{46}$$

The maximum value of the rate is attained when $d^2x_c/dt^2 = 0$; that is

$$vt = \frac{1}{B_0}\left[\left(\frac{B_0}{4\pi}\right)^{\frac{1}{2}} - B_1\right] \tag{47}$$

Introducing this expression in Equations (44) and (45), we obtain the maximum value of (dx_c/dt) and the corresponding conversion x_{cm} as

$$\left(\frac{dx_c}{dt}\right)_m = v(4\pi B_0)^{\frac{1}{2}} \exp\left[-\left(\frac{1}{2} - 2\pi \frac{B_1^2}{B_0}\right)\right] \tag{48}$$

$$x_{cm} = 1 - \exp\left[-\left(\frac{1}{2} - 2\pi \frac{B_1^2}{B_0}\right)\right] \tag{49}$$

If $B_0 < 4\pi B_1^2$, the reaction rate dx_c/dt declines monotonically with conversion.

Expressions (44) to (49) are specific instances of the general results embodied in Equations (31) to (33) which were derived independently of pore model. Equation (49) imposes the curious restriction (since $B_0 > 0$)

$$x_{cm} \leq 1 - e^{-\frac{1}{2}} \cong 0.393 \tag{50}$$

Experimental values of x_{cm} above 0.393 suggest deviations from the random pore model, assuming as always the absence of diffusional limitations and the independence of v from conversion.

Equation (44) implies that reactivity data alone can be used to determine $B_0 v^2$ and $B_1 v$ but not B_0, B_1, v individually. When the initial surface area is also available, then all three quantities B_0, B_1 and v can be determined. The determination of $B_0 v^2$, $B_1 v$ is best performed by nonlinear regression using Equation (44) or (46), depending on which form the data are available. A simpler but less accurate technique is to rewrite Equation (44) or (46) to accept straight line plotting.

It is recalled that the random pore model is not appropriate for large porosities. In fact, Dutta et al. (1977) have found that the char particles disintegrate to fragments at about $x_c = 0.8$. Therefore, comparisons with experimental data should not be carried out beyond a certain upper limit such as $x_c = 0.7$.

COMPARISONS WITH EXPERIMENTAL DATA

We consider first the applicability of the model-independent results concerning the existence of a master curve for $x_c(t)$ etc. Mahajan et al. (1978) have analyzed char reactivity data with oxygen, carbon dioxide, water and hydrogen by correlating the conversion with the dimensionless time $t/t_{0.5}$ up to conversion $x_c = 0.7$. They tested a linear, quadratic and cubic equation and found that the last gave the best correlation:

$$x_c = a(t/t_{0.5}) + b(t/t_{0.5})^2 + c(t/t_{0.5})^3$$

The coefficients a, b, c varied somewhat with the different gases. For a lignite char, PSOC 140, the best correlation was obtained for the reaction with oxygen and the worse for the reaction with carbon dioxide. In this particular case, $t_{0.5}$ was 29.6, 10.3 min for oxygen and carbon dioxide, respectively, indicating that the worse correlation with carbon dioxide may be due to incipient diffusional limitations. However, other possibilities exist. P. L. Walker has suggested two other possibilities, the inhibition of the carbon dioxide gasification reaction by hydrogen, which is difficult to control experimentally, and the sintering of the mineral catalysts, which would be more pronounced in the case of carbon dioxide because of the higher reaction temperatures. In the same paper by Mahajan et al. (1978), the conversion curves of another lignite char (PSOC 91) fitted very well a single master curve when plotted as functions of $t/t_{0.5}$. For another yet lignite char (PSOC 87) two $x_c(t)$ curves are presented, one for the raw char and another for the acid washed char. The two curves vary in shape, and the first does not exhibit the characteristic inflexion point ($d^2x_c/dt^2 = 0$) predicted by the theory. This suggests that the mineral catalysts may cause the surface velocity v to vary with conversion.

Dutta and Wen (1977) studied the gasification of several chars by oxygen at about 500°C and presented their data as dx_c/dt vs. $1 - x_c$ curves. For an IGT char No. 150, the rate data at several temperatures were found to fit well a single master curve by plotting $(dx_c/dt)/(dx_c/dt)_{x_c^*}$, where x_c^* was a fixed conversion level (for example, 0.2 or 0.4 or 0.7). With several chars it was observed that the conversion x_{cm}, where (dx_c/dt) attains its maximum, is approximately independent of temperature. Dutta et al. (1977) measured the gasification of the same chars by carbon dioxide at 840° to 1 100°C. Much of the data, especially at

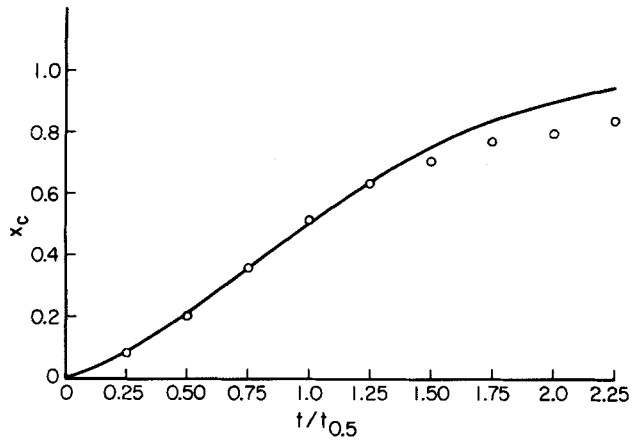

Figure 2. Comparison of theory with data from the gasification of a PSOC-91 char by O_2 (Mahajan et al., 1978)

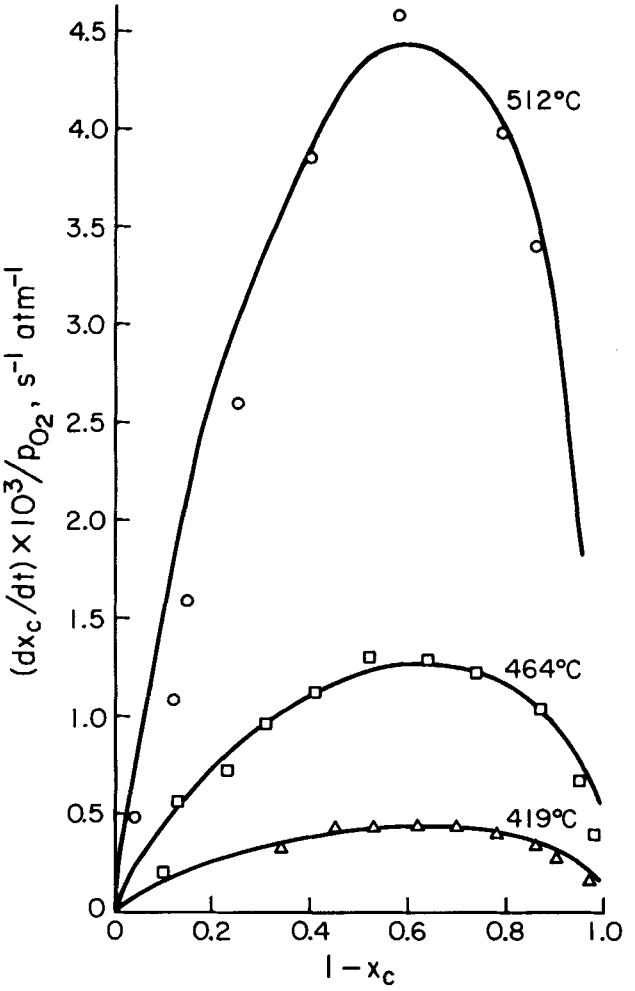

Figure 3. Comparison of theory with data from the gasification of a Hydrane Char No. 150 by O_2 (Dutta and Wen, 1977)

the higher temperatures, deviate considerably from the form of Equation (33). This deviation may be partially due to incipient diffusional limitations, inasmuch as for some of the experiments the half time $t_{0.5}$ was of the order of only 1 min (see Appendix).

The above comparisons show that much of the data, especially for the oxygen reaction and the lower temperatures, support the general principles embodied in Equations (31) to (33). Deviations were observed at the higher temperatures and for carbon dioxide reactant, indicating diffusional limitations or changes in the specific activity of the mineral catalysts.

We now proceed to test expressions (44) and (46) derived from the random capillary model. The comparison is restricted to data that are in satisfactory agreement with the general expressions (31) to (33). The normalized data from the gasification of a PSOC-91 char at different oxygen pressures (Mahajan et al., 1978) were fitted by linear least squares to Equation (44) rewritten in the form

$$\frac{1}{t''} \ln \frac{1}{1 - x_c(t'')} = A_0 t'' + A_1 \tag{51}$$

where A_0, A_1 are constants proportional to B_0, B_1. The regression utilized data up to $x_c = 0.70$, with the result $A_0 = 0.461$, $A_1 = 0.2353$ and a correlation coefficient 0.996. Figure 2 compares the data with the model prediction. The agreement is very good up to about $x_c = 0.7$, beyond which the calculated conversion exceeds the experimental.

Another set of comparisons was performed with the data of Dutta and Wen (1977) for gasification by oxygen of IGT char No. HT 155 and Hydrane Char No. 150. In both cases, linear regression was performed (up to $x_c = 0.7$) using equation (46) in the form

$$\left[\frac{1}{4\pi(1 - x_c)} \frac{dx_c}{dt}\right]^2 = A_0 \ln \frac{1}{1 - x_c} + A_1^2 \tag{52}$$

where A_0, A_1 are proportional to B_0, B_1. The results for the Hydrane Char No. 150 are compared with the experimental data in Figure 3. The values of the parameters were determined as follows:

T, °C	A_0	A_1^2	A_0/A_1^2
419	0.0062	0.00016	38.8
464	0.052	0.0015	34.7
512	0.65	0.013	50.0

Note that the theory predicts that A_0/A_1^2 should be independent of temperature. The agreement is very good, especially at the lower two temperatures. Good agreement was also obtained for IGT Char No. HT 155.

APPENDIX: APPROXIMATE CRITERIA FOR KINETIC CONTROL

Because of the wide pore size distribution and the small particle size of char, the description of mass transfer by an effective diffusion coefficient is not always feasible, and a more detailed consideration of the role of various pores may be necessary. To assess the possibility of diffusional limitations in char gasification, we replace the continuous pore size distribution (transitional pores and macropores) with a discrete one: R_1, ϵ_1; R_2, ϵ_2; R_3, ϵ_3. For the purpose of these calculations, we choose $R_1 = 5 \times 10^{-3}$ μm, $\epsilon_1 = 0.02$; $R_2 = 5 \times 10^{-2}$ μm, $\epsilon_2 = 0.02$; $R_3 = 0.5$ μm, $\epsilon_3 = 0.05$. Using expressions (23) to (28) and the approximate relation (7) between λ_i and ϵ_i, we calculate $L_1 = 3.7$ μm, $L_2' = 18.2$ μm. The latter value, which is the average length of R_2 pore segments between intersections with R_3 pores, suggests that the R_2 and R_3 pores are not well cross linked, at least for particles with $R_p \sim 100$ μm.

We will separately analyze diffusion and reaction in pores of different radii. Starting with the R_1 pores and using the reasoning that led to Equation (43), we obtain an approximate relation between the rate constant and the half time:

$$vt_{0.5} \simeq \left(\frac{2\pi}{\epsilon_1}\right)^{\frac{1}{2}} R_1$$

For a first-order reaction $r(c) = k_i c$, we obtain

$$k_i \simeq \left(\frac{2\pi}{\epsilon_1}\right)^{\frac{1}{2}} \frac{\rho_s R_2}{t_{0.5} c}$$

The diffusion length for the R_1 pores is not the particle radius but the average length between intersections with larger pores or the external particle surface. The later contribution is negligible for the R_1 pores; hence the diffusion length is L_1'. The rate $k_i c$ is in grams of carbon per unit surface area and time; therefore, the concentration c of the reactant gas obeys the equation

$$\mathcal{D}_{K1} \frac{d^2c}{dx^2} = \frac{2}{R_1} \frac{b}{12} k_i c \tag{A1}$$

where $\mathcal{D}_{K1}$ is the Knudsen diffusion coefficient, and b is a stoichiometric coefficient. To be concrete we shall consider the reaction $C + 0.5O_2 =$ carbon monoxide, where $b = 0.5$. The Thiele modulus for this situation is given by

$$\Phi_1 = \frac{L_1'}{2}\left(\frac{k_1}{12R_1\mathcal{D}_{K1}}\right)^{1/2} = \left(\frac{2\pi}{\epsilon_1}\right)^{1/4} L_1'\left(\frac{\rho_s}{48ct_{0.5}\mathcal{D}_{k1}}\right)^{1/2} \tag{A2}$$

Using the chosen values for $R_i\epsilon_i$, $t_{0.5} = 10$ min, c corresponding to 0.2 atmospheres and 500°C, $\rho_s = 2$ g/cm^3, we obtain $L_1' \cong 4.2$ μm, $\Phi_1 = 0.076$.

To examine the concentration gradient in the R_2 pores we note that these pores intersect both the R_3 pores and the external surface of the particle. The total number of intersections is

$$n_{23}\frac{4\pi}{3}R_{p0}^3 + \lambda_2 4\pi R_{p0}^2$$

while the total length of the R_3 pores is

$$2\lambda_2\frac{4\pi}{3}R_{p0}^3$$

Therefore, the mean length between intersections is obtained by dividing the total length by the total intersections

$$L_{2,\text{eff}} = \left[\pi\lambda_3(R_2 + R_3) + \frac{3}{2R_{p0}}\right]^{-1} \tag{A3}$$

or, using the low porosity approximation for λ_3

$$L_{2,\text{eff}} = \left[\frac{\epsilon_3}{2R_3^2}(R_2 + R_3) + \frac{3}{2R_{p0}}\right]^{-1} \tag{A4}$$

The reaction-diffusion equation for the R_2 pores is similar to (A1)

$$\mathcal{D}_{2,\text{eff}}\frac{d^2c}{dx^2} = \frac{2bk_i}{12R_2}(1 + \beta_2)c \tag{A5}$$

where $\mathcal{D}_{2,\text{eff}}$ is the effective diffusion coefficient, approximately given by the combination of Knudsen and bulk coefficients

$$\frac{1}{\mathcal{D}_{2,\text{eff}}} = \frac{1}{\mathcal{D}_{K2}} + \frac{1}{\mathcal{D}_{ij}}$$

The sink term includes a factor β_1 accounting for the reactive contribution of the R_1 pores intersecting a unit area of R_2 pores. Neglecting the intersections of R_1 pores with the external surface, we have

$$\beta_2 = \frac{\lambda_1 R_1}{\lambda_2 R_2}\frac{n_{12}}{n_{12} + n_{13}} = \frac{\epsilon_1(R_1 + R_2)}{R_1R_2\left(\epsilon_2\dfrac{R_1 + R_2}{R_2^2} + \epsilon_3\dfrac{R_1 + R_3}{R_3^2}\right)}$$

The Thiele modulus is now defined by

$$\Phi_2 = \frac{L_{2,\text{eff}}}{2}\left[\frac{k_i(1 + \beta_2)}{12R_2\mathcal{D}_{2,\text{eff}}}\right]^{\frac{1}{2}} \tag{A6}$$

with the assigned parameter values and $R_{p0} = 100$ μm, $\mathcal{D}_{ij} = 3$ cm^2/s we obtain $L_{2,\text{eff}} = 14.3$ μm and $\Phi_2 = 0.079$.

The calculation for the R_3 pores follows similar lines. The diffusion length, diffusion coefficient and reaction terms are R_{p0}, $\mathcal{D}_{ij}$, $(1 + \beta_3)\,k_ic$. The factor β_3 includes contributions of intersecting R_1 pores and R_2 pores:

$$\beta_3 = \frac{\lambda_1 R_1}{\lambda_3 R_3}\frac{n_{13}}{n_{12} + n_{13}} + (1 + \beta_2)\frac{\lambda_2 R_2}{\lambda_3 R_3}\frac{n_{23}}{n_{23} + \dfrac{3\lambda_2}{R_{p0}}}$$

As before, the relevant Thiele modulus is defined by

$$\Phi_3 = \frac{R_{p0}}{2}\left[\frac{k_i(1 + \beta_3)}{12R_3\mathcal{D}_{ij}}\right]^{\frac{1}{2}} \tag{A7}$$

so that the previous parameter values yield $\Phi_3 = 0.137$.

The criterion for chemical control is that $\Phi_1, \Phi_2, \Phi_3 < 0.3$. In the example taken, the criterion is satisfied. However, diffusional limitations would already appear for larger particles, for example, $R_p = 250$ μm.

NOTATION

B_0, B_1 = moments of probability density $\lambda(R)$, Equation (40) and (41)
c = concentration of reactant gas
$F(R)$ = defined by Equation (11)
k_i = surface reaction rate constant
l = length of pore axes per unit volume
$l_{0.5}$ = length characteristic of initial pore structure
L_c = characteristic length
L_i = mean length of R_i pore segment between intersections with $R_i, \ldots, R_n$ pores
L_i' = mean length of R_i pore segment between intersections with $R_{i+1}, \ldots, R_n$ pores
n' = number of pore intersections per unit pore length
n_{ij}' = number of intersections between R_i, R_j pores per unit length of R_i pore
n_{ij} = number of intersections between R_i, R_j pores per unit volume
$p(\cdot)$ = probability
$P(\cdot)$ = orientational probability density
q = increase in pore radius due to reaction
r = surface reaction rate
R, R_i = pore radius
R_*, R^* = smallest and largest pore radii
R_p = particle radius
t = time
t' = tv/L_c, dimensionless time
t'' = $t/t_{0.5}$, dimensionless time
$t_{0.5}$ = time to $x_c = 0.5$
v = reaction velocity
x_c = carbon conversion

Greek Letters

$\mathcal{D}_{ij}$ = bulk diffusion coefficient
$\mathcal{D}_{Ki}$ = Knudsen diffusion coefficient in R_i pores
ϵ = porosity
ϵ_T = total porosity
$\epsilon(R)$ = experimental pore size density function
θ = angle with the unit normal
λ = number of pore axes intersecting a unit area
$\lambda(R)$ = probability density function characterizing the porous medium
ρ_s = density of char excluding transitional and macropore volume
ϕ = azimuthal angle
Φ_i = Thiele modulus in R_i pores

Subscripts

o = initial value
m = value at the maximum of dx_c/dt

LITERATURE CITED

Dutta, S., C. Y. Wen, and R. J. Belt, "Reactivity of Coal and Char. 1. In Carbon Dioxide Atmosphere," *Ind. Eng. Chem. Process Design Develop.*, **16**, 20 (1977).

Dutta, S., and C. Y. Wen, "Reactivity of Coal and Char. 2. In Oxygen-Nitrogen Atmosphere," *ibid.*, **16**, 31 (1977).

Feng, C., and W. E. Stewart, "Practical Models for Isothermal Diffusion and Flow of Gases in Porous Solids," *Ind. Eng. Chem. Fundamentals*, **12**, 143 (1973).

Gan, H., S. P. Nandi, and P. L. Walker, Jr., "Nature of the Porosity in American Coals," *Fuel*, **51**, 272 (1972).

Gavalas, G. R., and K. A. Wilks, "Intraparticle Mass Transfer in Coal Pyrolysis," *AIChE J.*, **26**, 201 (1980).

Hashimoto, K., and P. L. Silveston, "Gasification: Part 1. Isothermal Kinetic Control Model for a Solid with a Pore Size Distribution," *ibid.*, **19**, 259 (1973).

Hippo, E., and P. L. Walker, Jr., "Reactivity of Heat-Treated Coals in Carbon Dioxide at 900°C," *Fuel*, **54**, 245 (1975).

Jenkins, R. G., S. P. Nandi, and P. L. Walker, Jr., "Reactivity of Heat-Treated Coals in Air at 500°C," *ibid.*, **52**, 288 (1973).

Johnson, M. F. L., and W. E. Stewart, "Pore Structure and Gaseous Diffusion in Solid Catalysts," *J. Catalysis*, **4**, 248 (1965).

Kendall, M. G., and P. A. P. Moran, *Geometrical Probability*, Charles Griffin, London, England (1963).

Linares-Solano, A., O. P. Mahajan, and P. L. Walker, Jr., "Reactivity of Heat-Treated Coals in Steam," *Fuel*, 58, 327 (1979).
Mahajan, O. P., R. Yarzab, and P. L. Walker, Jr., "Unification of Coal-Char Gasification Reaction Mechanisms," *ibid.*, 57, 643 (1978).
Mahajan, O. P., and P. L. Walker, Jr., "Effect of Inorganic Matter Removal from Coals and Chars on their Surface Areas," *ibid.*, 58, 333 (1979).
Petersen, E. E., "Reaction of Porous Solids," *AIChE J.*, 3, 443 (1957).
Simons, G. A., and M. L. Finson, "The Structure of Coal Char: Part I. Pore Branching," *Comb. Sci. Tech.*, 19, 217 (1979).
Simons, G. A., "The Structure of Coal Char: Part II. Pore Combination," *ibid.*, 19, 227 (1979).
Szekely, J., and J. W. Evans, "A Structural Model for Gas-Solid Reactions with a Moving Boundary," *Chem. Eng. Sci.*, 25, 1091 (1970).
Szekely, J., and J. W. Evans, "A Structural Model for Gas-Solid Reactions with a Moving Boundary—II," *ibid.*, 26, 1901 (1971).
Tomita, A., O. P. Mahajan, and P. L. Walker, Jr., "Reactivity of Heat-Treated Coals in Hydrogen," *Fuel*, 56, 137 (1977).

Manuscript received August 13, 1979; revision received February 13, and accepted February 29, 1980.

An Optimal Arrangement of Simultaneous Linearized Equations for General Systems of Interlinked, Multistaged Separators

R. HIDALGO S., A. CORREA V., A. GOMEZ M.
Instituto Mexicano del Petroleo, Mexico, Mexico D. F., Mexico
and
J. D. SEADER
University of Utah, Salt Lake City, Utah 84112

The simultaneous solution of all the equations for a general system of interlinked, multistaged separators is considered. The interlinks may be simple streams or reciprocal streams, and a particular separator may have bypassing streams (for example, pumparounds). Algorithms are developed that automatically arrange the linearized equations so that for a Newton-Raphson type of solution procedure using, for example, the Naphtali-Sandholm technique, a minimum or nearly minimum number of nonzero blocks occur outside the tridiagonal band so that computational memory and time requirements are minimized. The nonzero and nonidentity blocks are stored in a single vector of variable dimension.

SCOPE

In recent years, techniques of designing industrial plants with digital computers, as described by Crowe et al. (1971) and Seader et al. (1977), have been widely applied. Sometimes, such plants consist of complex arrangements of interlinked unit operation modules, each of which can be calculated as an independent unit. Two general approaches can be applied to the solution of the set of equations corresponding to an interlinked system. The first consists of solving the separate equations for each unit sequentially and iteratively and is called the sequential method. In the second procedure, called the simultaneous method, the complete set of equations for the system is solved. The sequential approach is usually adopted for designing processes because the approach offers great modularity; that is, each unit of the plant can be modeled separately. However, the simultaneous approach offers advantages for problems with a high degree of feedback or many recycle streams. Recycle problems are becoming more popular for ecological reasons and because of the energy and raw material crises.

The simultaneous method can involve a large set of nonlinear equations. Therefore, numerical methods of solving these equations must take advantage of the structure of the system in order to minimize computer memory requirements. For example, consider the general separation system of Sargent and Gaminibandara (1975) which performs the separation of n components as shown in Figure 1 (for simplicity, condensers and reboilers are not shown). This structure offers great flexibility, since column sections and streams can be developed by starting with a given processing scheme (analysis of a flow sheet) or can begin by looking for a good structure (synthesis). Any complex separation scheme obtained from the general one is represented by a set of nonlinear equations that can be solved using a Newton-Raphson technique. Such a set of equations exhibits a sparse structure with a number of nonzero block elements outside a tridiagonal band as presented in the case of interlinked distillation column systems by Stupin and Lockhart (1972), Browne, Ishii and Otto (1977), Tedder and Rudd (1978),

A. Correa V. is also at ESFM of Instituto Politécnico Nacional, Mexico City, Mexico.

0001-1541-80-2342-0585-$01.05.